Two-dimensional hybrid model of inductively coupled plasma sources for etching

Peter L. G. Ventzek, Timothy J. Sommerer,[a] Robert J. Hoekstra, and Mark J. Kushner[b]
Department of Electrical and Computer Engineering, University of Illinois, Urbana, Illinois 61801

(Received 15 March 1993; accepted for publication 1 June 1993)

Inductively coupled plasmas (ICPs) are currently being investigated as high density ($>10^{11}$–10^{12} cm^{-3}), low pressure (<1–20 mTorr) sources for semiconductor etching and deposition. We have developed a two-dimensional (r,z) hybrid model for ICP sources and have used the model to investigate $Ar/CF_4/O_2$ mixtures for etching applications. The simulation consists of electromagnetic, electron Monte Carlo, and hydrodynamic modules with an "off-line" plasma chemistry Monte Carlo simulation. The model produces the temporally and spatially dependent magnetic and electric fields (both inductively and capacitively coupled), plasma densities, and the energy resolved flux of ions and radicals to the substrate. We discuss results for densities, power deposition, and ion energies to the substrate as a function of position.

Plasma etching is moving toward reactors using lower pressures (<a few to 10 s mTorr), and having a low and controllable bias on the substrate.[1] These systems have less ion scattering, and a more anisotropic, less damaging flux of energetic ions to the wafer. Inductively coupled plasma (ICPs) using new coil configurations have recently been introduced which are capable of producing high density ($>10^{11}$–10^{12} cm^{-3}) plasmas at low pressure (<1–20 mTorr) over large wafers (200-mm diameter).[2–8] This configuration is shown in Fig. 1(a). The reactor is a squat cylinder with a dielectric roof. The roof-to-substrate height is 5–15 cm, and the plasma zone is 10–30 cm in diameter. The plasma is generated by an inductively coupled azimuthal electric field produced by a flat spiral coil antenna having a rectangular cross section. Applied voltage to the antenna at rf produces currents of a few to 10 s A through the coil and peak azimuthal electric fields in the plasma of a few of 10 s V cm^{-1}. In carefully designed reactors, the fractional amount of power which is capacitively coupled by the antenna into the plasma can be small, and the plasma potential can be quiescent. The substrate can also be independently biased by applying a rf potential. Multipole magnets can also be placed on the outer periphery of the chamber to produce a radial magnetic bucket. Plasma densities $>10^{11}$–10^{12} cm^{-3} have been measured in Ar and O_2 for power depositions of 100 s W–1 kW at gas pressures of 1–20 mTorr, with plasma potentials of 10–30 V.[2–8]

We have developed a computer model of the ICP reactor to investigate excitation mechanisms and the uniformity of ion energy fluxes to the substrate.[9] The two-dimensional (2D) (r,z) model is a hybrid simulation consisting of an electromagnetic module (EMM), an electron Monte Carlo Simulation (EMCS), a hydrodynamic-chemical kinetics simulation (HKS), and an off-line plasma chemistry Monte Carlo simulation. The model is conceptually a 2D analogue of the one-dimensional Monte Carlo-fluid model for rf discharges described in Ref. 10.

The simulation begins with the EMM by calculating the coil generated electric and magnetic fields [$E(r,z,\phi)$ and $B(r,z,\phi)$] in the plasma as a function of position and phase ϕ during the rf cycle. The method of solution is functionally the same as used by Yu and Girshick[11] in which we solve the complex wave equation

$$\nabla^2 E(r,z) = i\omega\mu_0\sigma(r,z)E(r,z), \tag{1}$$

where $E(r,z)$ is the complex amplitude of the azimuthal field, $\sigma(r,z)$ is the plasma conductivity, and we assume a purely sinusoidal field driven at frequency ω (rad/s). Equation (1) is solved within the plasma using the method of successive-over-relaxation (SOR). These fields are then

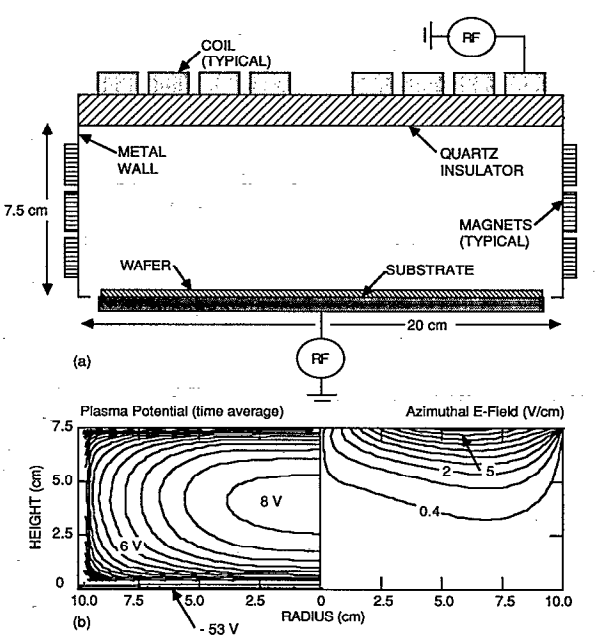

FIG. 1. (a) Schematic of the ICP reactor. (b) Time averaged plasma potential and amplitude of the azimuthal electric field. Selected contours have been removed for clarity.

[a]Present address: General Electric, Research and Development Center, P.O. Box 8, Schenectady, NY 12301.
[b]Author to whom correspondence should be addressed.

 0003-6951/93/63(5)/605/3/$6.00

used in the EMCS to advance electron trajectories to calculate the time averaged electron energy distribution, $f(\epsilon,r,z)$. This is obtained by averaging electron trajectories over $\simeq$50 rf cycles while including all pertinent collisions.[10] $f(\epsilon,r,z)$ is then used to calculate source functions for electron impact process, transport coefficients, and average electron energies as a function of (r,z). These quantities are then passed to the HKS.

The HKS integrates the continuity equations for the densities of all charged and neutral species, and solves Poisson's equation for the electrostatic plasma potential using the SOR method. Longitudinal and transverse transport coefficients are used to account for the effects of the confining multipole magnets. Since our mesh spacing is presently not fine enough to resolve the sheath at the surface of dielectrics at high plasma densities, we use an analytic sheath model placed between the last mesh point and the actual physical boundary. To extend the continuum portion of the model to lower pressures we limit diffusion speeds to the thermal velocities of the particles. When including a rf bias on the substrate, we calculate the electrostatic field as a function of phase during the rf cycle, $E_s(r,z,\phi)$. We account for the different effective areas of the electrodes by using a simple circuit having a blocking capacitor, and calculate the dc bias generated on the substrate. The surfaces of the chamber are specified as being either metal or dielectric. The potential boundary condition on the surface of the dielectric is obtained by specifying the potential on the "backside" of the dielectric, and using the calculated surface charge density and Gauss' law at the boundary. An acceleration technique is used to speed the convergence of the HKS by predicting future species densities based on recent time histories of those densities.[12] After the HKS, $\sigma(r,z)$ is cycled back to the EMM; and $E_s(r,z,\phi)$ and species densities are cycled back to the EMCS to iterate through the model until convergence. Typically 10–20 iterations are required.

Energy distributions for ions and radicals are not obtained in the model just described. To obtain this information as a function of (r,z), we use an "off-line" plasma chemistry Monte Carlo Simulation (PCMCS) which uses electron impact sources and electric fields from the EMCS and HKS. The PCMCS launches pseudoparticles for ions and radicals based on the source functions, and advances their trajectories using the imported fields. All pertinent collisions and chemical reactions are included on a particle-mesh basis using a modified null cross-section technique.[10] Heavy particle reactions are taken from Sommerer and Kushner,[10] and Plumb and Ryan.[13]

A unique feature of the HKS is a semi-implicit solution of Poisson's equation which allows us to take time steps 10–100 s times larger than the dielectric relaxation time.[14] The solution uses a predicted charge density at a future time $(t+\Delta t)$ to obtain the potential which is used to advance the densities from the present to that future time

$$\nabla^2\phi(t+\Delta t)=-\frac{1}{\epsilon_0}\left[\rho(t)+\Delta t\frac{d\rho}{dt}(t)\right], \tag{2a}$$

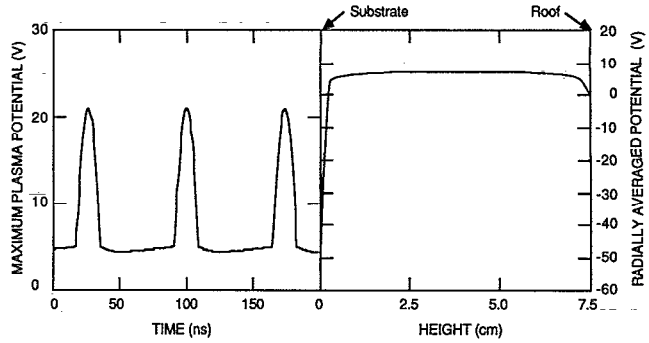

FIG. 2. (a) Maximum plasma potential as a function of time. (b) Time averaged plasma potential ($r=0$) as a function of height.

$$\frac{d\rho}{dt}=\sum_i eq_i\nabla(D_i\nabla N_i+q_iN_i\mu_i\nabla\phi). \tag{2b}$$

In Eq. (2), ϕ is the potential, ρ is the charge density, q_i is the charge (1 or -1), N_i is the density, D_i is the diffusion coefficient, and μ_i is the mobility of species i. Since local reactions are conservative with respect to ρ, $d\rho/dt$ in Eq. (2) contains only transport terms. We can rewrite Eq. (2) as

$$\nabla^2\phi(t+\Delta t)+\frac{1}{\epsilon_0}\Delta t\sum_i eq_i\mu_i(\nabla N_i\nabla\phi+N_i\nabla^2\phi)$$

$$=-\frac{\rho(t)}{\epsilon_0}-\frac{1}{\epsilon_0}\Delta te\sum_i q_i(\nabla D_i\nabla N_i), \tag{3}$$

which is the form we solve. This form is conceptually Lagrangian since the effect of the added terms on the left-hand side of Eq. (3) is to distort the computational mesh to eliminate any change in charge density due to drift.

The model was applied to analyzing ICP reactors having $Ar/CF_4/O_2=85/12/3$ mixtures as used in the etching of silicon dioxide. The gas pressure is 15 mTorr and the total power deposition is 900 W. A rf bias of 75 V (amplitude) is applied to the substrate at 13.56 MHz. There is no capacitive coupling from the coil. The radial magnetic bucket has a peak field of 1.5 kG at the periphery. The time averaged azimuthal electric field E_θ and plasma potential are shown in Fig. 1(b). The peak plasma potential (measured with respect to ground at the sidewalls) as a function of time, and the time averaged plasma potential are shown in Fig. 2. E_θ is toroidal shaped[2] with a maximum value of $\simeq$5 V cm^{-1} under the dielectric, which is approximately the same E/N measured in Ar plasmas.[7] E_θ is asymmetric due to the higher electron density and smaller skin depth at small radii. The peak electron temperature of $\simeq$3 eV, is also commensurate with that measured in Ar plasmas.[7] The time averaged plasma potential is radially flat (maximum value $\simeq$8 V) due to the confining effects of the magnetic bucket, and approximately one-half to two-thirds that without the bucket.[4] The dc bias is -53 V with a minimum excursion of the plasma potential of -128 V. The maximum plasma potential oscillates between $\simeq$6 and 20 V.[15]

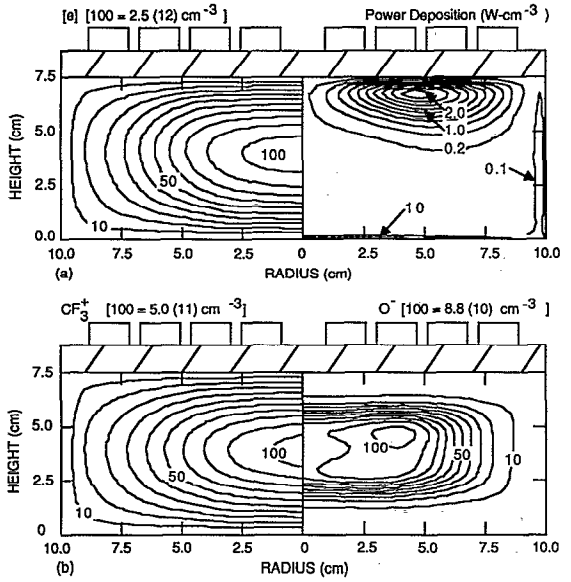

FIG. 3. Calculated plasma parameters. (a) Electron density and time averaged power deposition. (b) CF_3^+ and O^- densities. Selected contours have been removed for clarity.

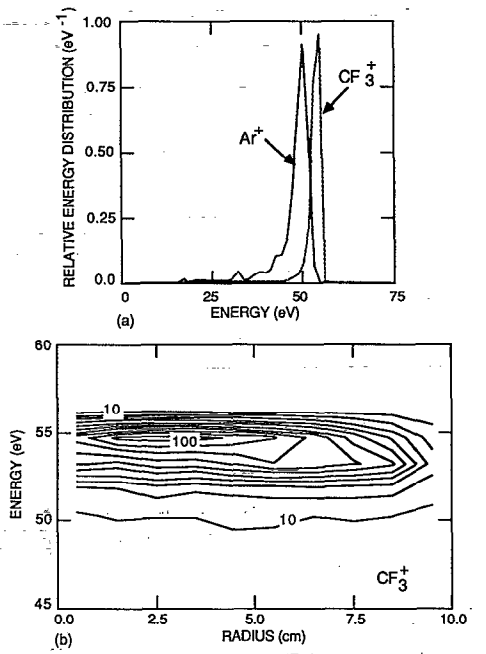

FIG. 4. Ion energy distributions incident on the substrate. (a) Radially averaged values for Ar^+ and CF_3^+. (b) Radially dependent energy distribution for CF_3^+.

Time averaged power deposition and electron density as a function of position are shown in Fig. 3(a). The power deposition from E_θ is the toroidally shaped region under the top dielectric. Power deposition from the rf bias is dominantly near the wafer and sidewalls, and consists primarily of ion acceleration. The peak electron density exceeds 10^{12} cm^{-3} (in agreement with experiments on a power/volume basis[7]) and has a fairly uniform radial profile due to the confining effects of the magnetic bucket, as shown by probe measurements.[6] The densities of CF_3^+ and O^- are shown in Fig. 3(b). The O^- ions pool at the peak of the plasma potential since they are near ambient temperature. A small amount of noise in the O^- density is caused by $\simeq$0.05 V noise in the plasma potential resulting from the Monte Carlo generated sources. We find that the electronegativities of low pressure, high plasma density discharges are lower than conventional higher pressure RIE discharges. This results from the production of negative ions scaling as $[e]N$ (N is the neutral gas density) whereas the destruction mechanism scales as $[N^-][N^+]$. Therefore low pressures and high plasma densities favor destruction processes over production processes.

Calculated energy distributions for Ar^+ and CF_3^+ ions as they strike the substrate are shown in Fig. 4. The CF_3^+ ions undergo only elastic collisions and so the maximum CF_3^+ energy is somewhat higher than the Ar^+. Their energy distributions are shifted by $\simeq$50 V by transport through the nearly collisionless sheath. The radial distribution of ion energies is fairly uniform.

In conclusion, we have developed a 2D hybrid model for ICP reactors. We have used the model to investigate plasma densities and particle distributions incident on the wafer in $Ar/CF_4/O_2$ gas mixtures. Plasma densities in excess in 10^{12} cm^{-3} are predicted for a power depositions of 500–1000 W. We find that ion energies arriving at the substrate are fairly uniform as a function of radius, and have energies near the dc bias.

The authors would like to thank M. Barnes, J. Keller, J. O'Neill, T. Wicker, J. Cook, and A. Wendt for discussions on ICPs, and H. Pak and M. Riley for discussions on acceleration techniques. This work was supported by IBM East Fishkill Facility, LAM Research Corp., Semiconductor Research Corp., National Science Foundation, and the University of Wisconsin ERC for Plasma Aided Manufacturing.

[1] J. Asmussen, J. Vac. Sci. Technol. A 7, 883 (1989).
[2] J. Keller, M. S. Barnes, and J. C. Forster, Proceedings of the 42th Gaseous Electronics Conference, Urbana, IL, 1990 (unpublished), paper NA-5.
[3] J. Hopwood, Plasma Sources Sci. Technol. A **1**, 109 (1992).
[4] J. A. O'Neill, M. S. Barnes, and J. H. Keller, J. Appl. Phys. **73**, 1621 (1993).
[5] M. S. Barnes, J. C. Forster, and J. H. Keller, Appl. Phys. Lett. **62**, 2622 (1993).
[6] J. Hopwood, C. R. Guarnieri, S. J. Whitehair, and J. J. Cuomo, J. Vac. Sci. Technol. A **11**, 147 (1993).
[7] J. Hopwood, C. R. Guarnieri, S. J. Whitehair, and J. J. Cuomo, J. Vac. Sci. Technol. A **11**, 152 (1993).
[8] A. E. Wendt, L. J. Mahoney, and J. L. Shohet, Proceedings of the 45th Gaseous Electronics Conference, Boston MA, 1992 (unpublished), paper LB-5.
[9] M. J. Kushner, T. J. Sommerer, and S. J. Choi, *Conference Record of the 1992 IEEE International Conference on Plasma Science* (IEEE, New York, 1992), p. 178.
[10] T. J. Sommerer and M. J. Kushner, J. Appl. Phys. **71**, 1654 (1992).
[11] B. W. Yu and S. L. Girshick, J. Appl. Phys. **69**, 656 (1991).
[12] H. Pak and M. Riley, in Ref. 8, paper BB-5.
[13] I. C. Plumb and K. R. Ryan, Plasma Chem. Plasma Proc. **6**, 11 (1986).
[14] M. S. Barnes, T. J. Colter, and M. E. Elta, J. Appl. Phys. **61**, 81 (1987).
[15] A video animation of the plasma potential (r,z,t) is available from the authors. Enclose a standard VHS cassette with your request.